Superantigen Binding to a T Cell Receptor β Chain of Known Three-dimensional Structure

By Emilio L. Malchiodi,* Edward Eisenstein,*‡ Barry A. Fields,* Douglas H. Ohlendorf,§ Patrick M. Schlievert,‖ Klaus Karjalainen,¶ and Roy A. Mariuzza*

*From the *Center for Advanced Research in Biotechnology, University of Maryland Biotechnology Institute, Rockville, Maryland 20850; ‡Department of Chemistry and Biochemistry, University of Maryland, Baltimore County, Maryland 21228; §Department of Biochemistry and ‖Department of Microbiology, University of Minnesota Medical School, Minneapolis, Minnesota 55455; and ¶Basel Institute for Immunology, Postfach CH-4005, Basel, Switzerland*

Summary

The three-dimensional structure of an unglycosylated T cell antigen receptor (TCR) β chain has recently been determined to 1.7 Å resolution. To investigate whether this soluble β chain (murine Vβ8.2Jβ2.1Cβ1) retains superantigen (SAG)-binding activity, we measured its affinity for various bacterial SAGs in the absence of MHC class II molecules. Dissociation constants (K_Ds) were determined using two independent techniques: surface plasmon resonance detection and sedimentation equilibrium. Specific binding was demonstrated to staphylococcal enterotoxins (SEs) B, C1, C2, and C3 and to streptococcal pyrogenic exotoxin A (SPEA), consistent with the known proliferative effects of these SAGs on T cells expressing Vβ8.2. In contrast, SEA, which does not stimulate Vβ8.2-bearing cells, does not bind the recombinant β chain. Binding of the β chain to SAGs was characterized by extremely fast dissociation rates (>0.1 s^{-1}), similar to those reported for certain leukocyte adhesion molecules. Whereas the β chain bound SEC1, 2, and 3 with K_Ds of 0.9–2.5 μM, the corresponding value for SEB was ~140 μM. The much weaker binding to SEB than to SEC1, 2, or 3 was surprising, especially since SEB was found to actually be 3- to 10-fold more effective, on a molar basis, than the other toxins in stimulating the parental T cell hybridoma. We interpret these results in terms of the ability of SEC to activate T cells independently of MHC, in contrast to SEB. We have also measured SE binding to the glycosylated form of the β chain and found that carbohydrate apparently does not contribute to recognition, even though the N-linked glycosylation sites at Vβ8.2 residues Asn24 and Asn74 are at or near the putative SAG-binding site. This result, along with the structural basis for the Vβ specificity of SEs, are discussed in relation to the crystal structure of the unglycosylated β chain.

Antigen recognition by T lymphocytes is mediated by highly diverse cell surface glycoproteins known as T cell receptors (TCRs)[1]. In addition to recognizing peptide antigens complexed with products of the MHC complex, TCRs interact with a class of molecules known as superantigens (SAGs), which stimulate T cells bearing particular Vβ regions, largely irrespective of the peptide/MHC specificity of the TCR (1–3). SAGs include self antigens, such as the minor lymphocyte stimulating antigens (Mls) encoded by endogenous murine retroviruses, as well as foreign antigens, such as staphylococcal and streptococcal pyrogenic toxins.

T cell stimulation by SAGs is generally thought to require the participation of MHC class II molecules (4–8), which bind some bacterial SAGs with affinities in the micromolar range (9–12). Most current models assume that SAGs activate T cells by simultaneously binding class II molecules on APC and the Vβ element on T cells (1–3, 13). Recently, however, through the use of class II knockout mice, staphylococcal enterotoxin C (SEC) and staphylococcal enterotoxin E (SEE) have been shown to activate T cells

[1] *Abbreviations used in this paper:* APC, antigen-presenting cell; βCHO, glycosylated β chain; βmut, unglycosylated β chain; HBS, Hepes-buffered saline; K_D, dissociation constant; Mls, minor lymphocyte stimulating antigen; r, correlation coefficient; RU, response unit; SAG, superantigen; SEA, staphylococcal enterotoxin A; SEB, staphylococcal enterotoxin B; SEC, staphylococcal enterotoxin C; SEE, staphylococcal enterotoxin E; SPEA, streptococcal pyrogenic exotoxin A; TCR, T cell antigen receptor.

independently of MHC (14). The response resembled the conventional class II-associated one in that T cells expressing the same Vβ gene segment were selectively stimulated. However, T cell activation by SEC and SEE in MHC-deficient mice was not followed by deletion of clones bearing the relevant Vβ element. Thus, MHC-independent T cell activation may produce certain physiological consequences which are different from those associated with MHC-dependent activation.

To investigate the biochemical basis of T cell activation by SAGs, we have measured the binding of various bacterial toxins to a soluble murine TCR β chain (Vβ8.2Jβ2.1 Cβ1) in the absence of MHC class II molecules. As we have recently determined the three-dimensional structure of this β chain to atomic resolution (15), this represents an excellent system for delineating TCR-SAG interactions. We show that the reactivity of this β chain toward different toxins is consistent with their effects on the parental T cell hybridoma. We also find that the ability of certain bacterial SAGs to activate T cells independently of MHC correlates with the relatively high affinity of these particular toxins for the isolated β chain. By measuring the affinity of glycosylated and unglycosylated forms of the β chain for SEs, we have been able to directly assess the contribution of carbohydrate to SAG binding. Finally, the identification of amino acid residues on the putative SAG-binding surface of the Vβ8.2 domain which are conserved in other Vβ domains with similar or different toxin reactivities provides insights into the structural basis of TCR recognition by SAGs.

Materials and Methods

Superantigens. Purified SEA, SEB, SEC1, SEC2 and SEC3 were purchased from Toxin Technology, Inc. (Sarasota, FL). Streptococcal pyrogenic exotoxin A (SPEA) was prepared as described (16).

Recombinant TCR Proteins. The soluble αβ TCR used is a chimeric molecule in which the V and extracellular C regions of both α and β chains were fused with immunoglobulin Cκ regions (17). The TCR (designated 14.3.d) is specific for a hemagglutinin peptide of influenza virus (HA 110-120) in the context of I-E^d and utilizes the Vα4.1Jα2B4/Vβ8.2Jβ2.1 gene combination (18). The chimeric protein is assembled and secreted as a functional, glycosylated VαCαCκ/VβCβCκ heterodimer by J558L myeloma cells transfected with the recombinant genes (17). Affinity purification using the anti-mouse Cκ monoclonal antibody 187.1 (19) was carried out as described (17).

Glycosylated 14.3.d VβCβ chain (βCHO) was derived from the VαCαCκ/VβCβCκ heterodimer by treatment with papain, which was found to selectively degrade the α chain as well as both Cκ domains (20). In a typical preparation, αβ heterodimer at a concentration of 2 mg/ml in 0.1 M KPO_4, pH 7.2, was digested for 35 min at 37°C with papain (Worthington) at an enzyme/substrate ratio of 1:500 in the presence of 1.25 mM EDTA and 1.5 mM 2-mercaptoethanol. The reaction was terminated by the addition of *N*-ethylmaleimide to a final concentration of 10 mM.

Unglycosylated VβCβ chain (βmut) was obtained by elimination of four out of five potential N-linked glycosylation sites through site-directed mutagenesis and introduction of a termination codon at the end of the first C region exon of the β chain (15). Asparagines at positions 24, 74, and 121 (numbering according to reference 21) were mutated to glutamine, while the glycosylation site at position 236 was eliminated by mutation of Ser238 to valine. The βmut chain was produced in J558L cells and affinity purified using the anti-mouse Cβ monoclonal antibody H57-597 (15, 22). The unmutated N-linked glycosylation site at position Cβ 186 was used in <10% of the chains, as judged by SDS-PAGE.

The bacterially produced Vα domain of a TCR (designated 1934.4) specific for the NH_2-terminal nonapeptide of myelin basic protein presented by I-A^u (23) was kindly provided by Dr. E. S. Ward (Southwestern Medical School, Dallas, TX). The His_6-tagged protein was purified by Ni^{2+}-NTA agarose and anion exchange chromatography as described (23, 24).

BIAcore Analysis. The interaction of soluble TCR fragments with immobilized SAGs was monitored with a BIAcore instrument (Pharmacia Biosensor, Uppsala, Sweden). All proteins were purified by gel filtration on a Superose 12 FPLC column (Pharmacia) before use to eliminate aggregated material that could interfere with affinity measurements (25, 26). Typically, <5% of the SAG or TCR preparations eluted at or near the void volume. SAGs were coupled to the dextran matrix of CM5 sensor chips (Pharmacia) using the Amine Coupling Kit as described (27). SEC1, SEC2, SEC3, SEB, and SEA, which have isoelectric points above 7.0 (16), were dialyzed against 10 mM sodium acetate, pH 5.5. SPEA, whose isoelectric point is ~5.0 (16), was dialyzed against 10 mM sodium acetate, pH 4.2. Protein concentrations ranged from 50 to 150 μg/ml. The activation and immobilization periods were set to between 2 and 7 min to couple the desired amount of SAG. Recombinant TCR fragments were dialyzed against Hepes-buffered saline (HBS) containing 150 mM NaCl, 0.005% Surfactant P-20 (Pharmacia), 10 mM Hepes, pH 7.5; dilutions were made in the same buffer. All binding experiments were performed at 25°C. Dissociation was carried out in HBS. Flow rates are given in the figure legends. Pulses of 10 mM HCl were used to regenerate the surfaces. Runs were analyzed using the software BIAevaluation 2.0 (Pharmacia). Dissociation constants (K_Ds) were determined under equilibrium binding conditions using Scatchard analysis (28). Standard deviations for three or more independent determinations were <8%.

Sedimentation Equilibrium. Equilibrium sedimentation of the βmut chain, the various SAGs, and their mixtures were performed with a Beckman XL-A Optima analytical ultracentrifuge using a four-hole, An-55 rotor. All experiments were performed between 20–25°C at rotor speeds of between 22,000 to 30,000 rpm. The molar extinction coefficients used were: βmut, 43,200 $M^{-1}cm^{-1}$; SEB, 40,500 $M^{-1}cm^{-1}$; SEC1, 34,200 $M^{-1}cm^{-1}$; SEC2, 34,200 $M^{-1}cm^{-1}$; SEC3, 34,200 $M^{-1}cm^{-1}$; SPEA, 29,900 $M^{-1}cm^{-1}$. The concentration distributions of the samples at sedimentation equilibrium were acquired either as a single measurement or as an average of 25 measurements of absorbance at each radial position, with nominal spacing of 0.001 cm between radial positions. Samples were prepared by dialysis against either 50 mM Tris-HCl, pH 7.0, or 0.1 M sodium phosphate, pH 7.2. Partial specific volumes for the β chain and the toxins were assumed to be 0.73 ml/mg, and solvent densities were determined pychnometrically.

Equilibrium sedimentation data on the individual β chain and individual SAGs obtained either at two different rotor speeds or two initial protein concentrations were analyzed for average molecular weights in terms of a single, homogeneous species according to

$$c_r = B + c_m \exp\left[M(1 - \nu\rho)\omega^2 (r^2 - r_m^2)/2RT\right] \quad (1)$$

where c_r is the concentration of the protein at a given radial position, c_m is the concentration of the protein at some reference position (e.g., the meniscus), M is the molecular weight, ν is the partial specific volume, ρ is the solvent density, ω is the angular velocity, r is the radial position in centimeters from the center of rotation, r_m is the distance in centimeters from the center of rotation to the meniscus, R is the gas constant, T is the absolute (Kelvin) temperature, and B is a correction term for a nonzero baseline.

Equilibrium constants for the association of the β chain and SAGS were calculated from the data obtained at sedimentation equilibrium according to

$$c_r = B + c_{m,R}\exp[M_R(1-\nu r)\omega^2(r^2-r_m^2)/2RT] + (c_{m,T})\exp[M_T(1-\nu r)\omega^2(r^2-r_m^2)/2RT] + (c_{m,R})(c_{m,T})/K_D\exp[M_C(1-\nu\rho)\omega^2(r^2-r_m^2)/2RT] \quad (2)$$

where $c_{m,R}$ is the concentration of receptor at the reference position, $c_{m,T}$ is the concentration of the toxin at the reference position, M_R and M_T are the molecular weights of the βmut chain and SAGs as determined in separate sedimentation equilibrium experiments, M_C is the molecular weight of the complex, and K_D is the dissociation constant for the various β chain-SAG interactions. Parameters were evaluated using nonlinear least-squares analysis (29), or by using a modified version of IGOR (Wavemetrics, Lake Oswego, OR) running on a Macintosh computer (30, 31). Data for two different concentrations or two rotor speeds were analyzed simultaneously as a test for homogeneity and reversibility (32) and to constrain confidence intervals for the parameter values (33). Errors on K_Ds were ~20% of parameter values.

T Cell Stimulation Assay. T cell stimulation was monitored by the release of IL-3 as previously described (34). Briefly, 5×10^4 irradiated (10,000 rad) A20 APC were preincubated with different concentrations of SAGs or positive control peptide (HA 110-119) in 100-μl volumes for 2 h in 96-well plates. Thereafter, 2×10^4 14.3.d T cell hybridoma cells were added in 100-μl volumes and supernatants were harvested 20 h later for assay of IL-3 activity. Proliferation of the IL-3–dependent cell line DA-1 was measured 26 h later using [^{3}H]thymidine. All measurements were done in duplicate in the presence of 5% FCS in IMDM culture media.

Results

The Binding of Soluble TCR Components to SAGs Is Characterized by Rapid Association and Dissociation Rates. To analyze the interaction of recombinant TCR molecules with SAGs by BIAcore, SAGs were coupled directly to the dextran matrix through primary amine groups of the proteins (27). Injection of different concentrations of 14.3.d αβ TCR, βCHO, and βmut over SEC1 gave concentration-dependent binding (Fig. 1, *A*, *B*, and *C*, respectively) that can be distinguished from the profile obtained when SEA was immobilized (Fig. 1 *E*). Results similar to those for SEC1 were obtained when SEC2, SEC3, and SPEA were coupled to the matrix (not shown). These data are in agreement with the ability of SEC and SPEA, but not SEA, to stimulate Vβ8.2-bearing T cells (2). Surprisingly, the binding to SEB, which is also known to activate cells expressing Vβ8.2 (2), appeared markedly weaker: whereas injection of 8 μM βmut over 4,000 response units (RU) of immobilized SEC1 produced a total response (specific and nonspecific; see below) of ~1,750 RU (Fig. 1 *C*), injection of the same concentration of β chain over 4,000 RU of immobilized SEB resulted in a response of only about 400 RU (Fig. 1 *F*). Similarly, injection of 8 μM αβ TCR over SEB produced a response of only ~200 RU (Fig. 1 *G*), indicating that the weak interaction of βmut with this toxin is not due to the absence of carbohydrate or of α chain. Injection of 8 μM 1934.4 Vα over SEC1 produced a response (Fig. 1 *D*) similar to that observed after injection of βmut over SEA (Fig. 1 *E*).

Efforts to examine binding in the reverse orientation (i.e., with TCR components on the sensor surface and SAGs in solution) were not successful. In the case of αβ TCR, although binding of SEC was detectable, baseline drift precluded quantitative analysis; similar difficulties have been reported for the binding of SEB to an immobilized human TCR (12). In the case of βCHO and βmut, no binding of any SAG could be detected, implying that immobilization of the β chain through amine groups led to its inactivation, as described in other systems (26). These difficulties prompted us to measure β chain-SAG interactions by sedimentation equilibrium (see below), which does not require ligand immobilization.

When 8 μM αβ TCR were injected over SEC1, SEC2, SEC3, and SPEA, the response occurred in two distinct phases: a fast initial increase of ~800 RU, followed by a much slower increase of ~300 RU (Fig. 1 *A*, for the case of SEC1). When buffer flow was reestablished, the response dropped in two phases: a fast initial drop of ~800 RU within 4 s, followed by a slower decrease over the remaining 300 RU. We attribute the slowly dissociating phase to the presence of multimeric aggregates of αβ TCR which bind with high avidity, even though the protein had been purified by size exclusion chromatography. It has been shown that even small amounts of aggregated material (<2%), which could form during the concentration step after gel filtration, can produce this type of biphasic dissociation (25, 26). On the other hand, when βCHO or βmut were injected over SEC1, SEC2, SEC3, and SPEA, equilibrium binding levels were reached within seconds (Fig. 1, *B* and *C*). Upon completion of the injections, the responses dropped rapidly as well (>90% decrease within the first 4 s in the case of βmut dissociating from SEC1; Fig. 1 *C*). Because βCHO and βmut displayed relatively simple kinetic behavior, and because the reactivity profiles of isolated β chain and αβ heterodimer toward SEC, SPEA, and SEB had been found to be qualitatively indistinguishable, all subsequent measurements were carried out with βCHO or βmut. It is worth noting that the monodisperse behavior of the β chain (see also below) is consistent with its ability to crystallize: whereas both βCHO and βmut have yielded x-ray diffraction quality crystals, we were unable to crystallize the αβ heterodimer (15, 20).

The kinetics of the binding of soluble TCR components to SAGs were too fast to be accurately measured, although the association and dissociation rate constants may be estimated at >100,000 $M^{-1}s^{-1}$ and >0.1 s^{-1}, respectively.

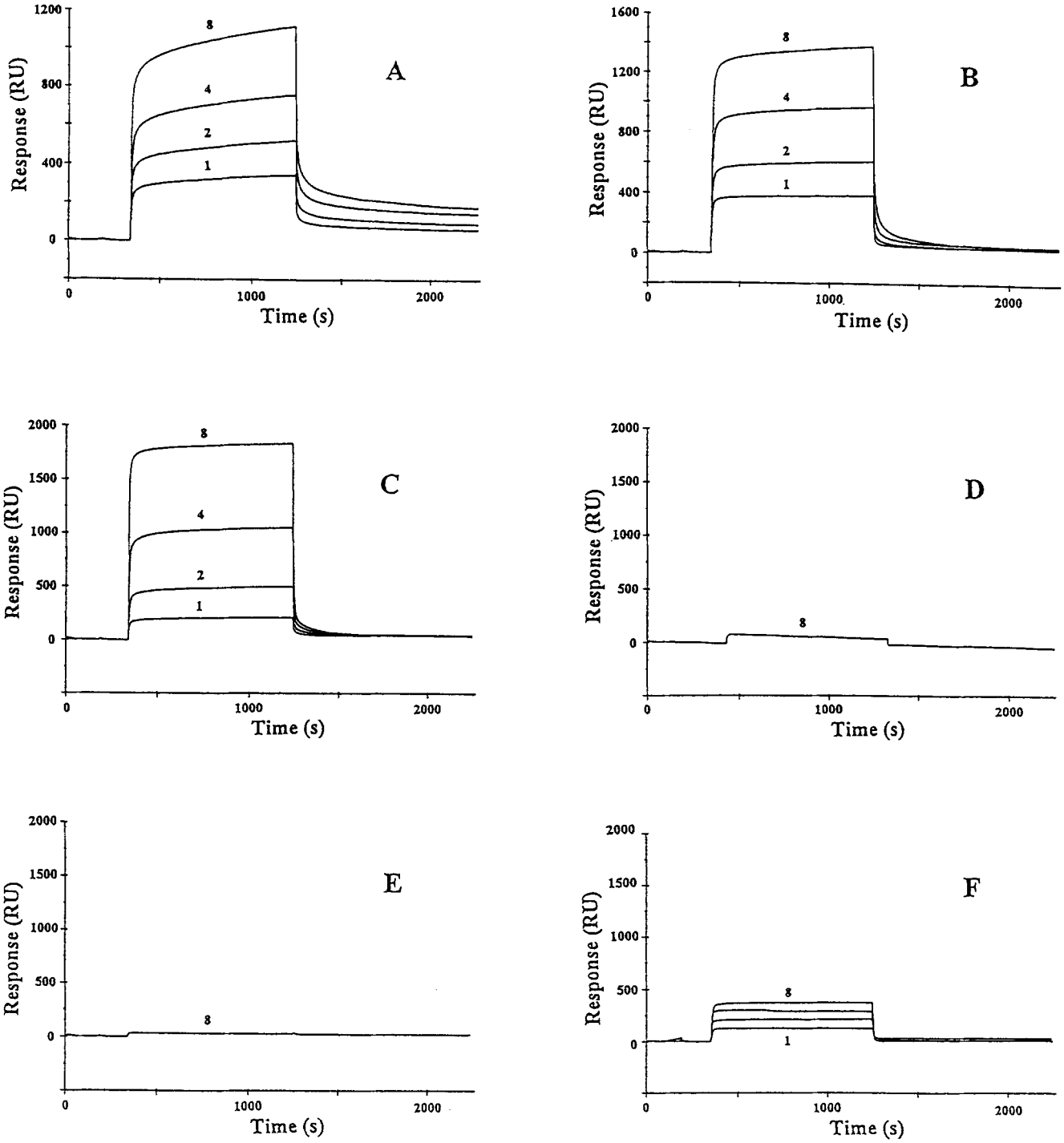

Consequently, affinities were determined under equilibrium binding conditions as described below.

Glycosylated and Unglycosylated TCR β Chains Bind SEC and SPEA with Micromolar Affinities. Conditions for equilibrium binding analysis were chosen on the basis of the kinetic behavior of this system (Fig. 1). Approximately 2,000 RU of each SAG were immobilized and buffer flow rates were set at 5 μl/min to avoid diffusion-limited reactions (28). Each β chain was injected over the surface for 20 s and report points for Scatchard analysis were taken 10 s after injection (Fig. 2). To estimate apparent K_Ds, decreasing concentrations (64, 32, 16, 8, 4, 2, and 1 μM) of βCHO or βmut were injected over SEA, SEC1, SEC2, SEC3, and SPEA. To estimate the increase in RU resulting from the nonspecific effect of protein on the bulk refractive index, binding of βCHO and βmut to a control surface with no immobilized ligand were also measured (Fig. 2 *A*). βCHO and βmut showed the same behavior over SEA as over the

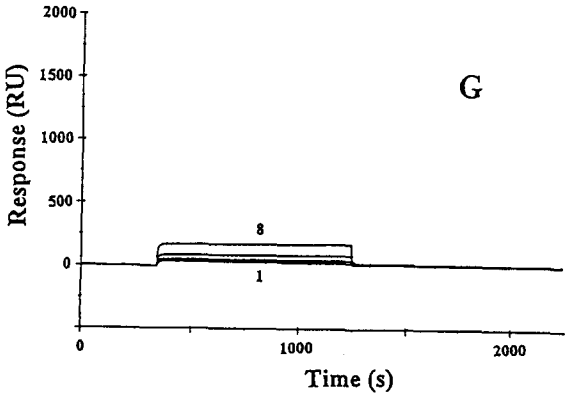

Figure 1. Concentration-dependent binding of soluble TCR components to immobilized SAGs. Binding to SEC1 by soluble αβ TCR (*A*), βCHO (*B*), βmut (*C*), and Vα (*D*) was recorded at the concentrations indicated (μM). Similar profiles were obtained when SEC2, SEC3 and SPEA were immobilized. In *E* and *F*, βmut was injected over SEA and SEB, respectively. In (*G*), αβ TCR was injected over SEB. For each SAG, 3,000–5,000 RU were immobilized. The buffer flow rate was 2 μl/min and TCR components were injected for 15 min. Dissociation was carried out for 15 min with HBS and the surfaces were regenerated by injection of 10 mM HCl between assays. Responses are given as increases over baseline values.

control surface. As an additional control for nonspecific binding, the same concentrations of an irrelevant protein, BSA, were injected over a surface with no protein immobilized (Fig. 2 *C*). As can be seen, the response to 32 μM BSA is comparable to the response to 64 μM βmut. Taking into account that the molecular mass of BSA is roughly twice that of βmut (66.2 versus 26.4 kD), and that there is a linear relationship between the mass of bound protein and the measured RU (35), it is apparent that both proteins give similar nonspecific effects on the bulk refractive index. When BSA was injected over a surface with SEC1, the signals were similar to those in Fig. 2 *C*, and much lower than the responses to equivalent masses of βmut (Fig. 1 *B*).

The specific binding of βCHO and βmut to immobilized SAGs was calculated as the difference between the responses on the SAG-derivatized and control surfaces. Plots of these data indicated that the binding of β chain to SEC1, SEC2, SEC3, and SPEA was saturable, as shown in Fig. 3, *A* and *C* for the interaction of βmut with SEC1 and SPEA, respectively. A Scatchard plot for the binding of βmut to SEC1 was linear (correlation coefficient [*r*] = 0.99) and gave a K_D of 19.8 μM. The predicted maximum specific binding was 1980 RU, while the amount of immobilized SEC1 was 2050 RU. Since SEC1 and βmut have similar molecular masses (27.5 and 26.4 kD, respectively), this indicates that nearly all the SEC1 and βmut in the assay were available for binding. The results for SPEA are shown in Fig. 3, *C* and *D*; a K_D of 6.2 μM was obtained. Similar analyses were carried out for the binding of βmut to SEC2 and SEC3, and for the binding of βCHO to SEC1, SEC2, and SEC3.

The results of these experiments are summarized in Table 1. The apparent K_Ds for the binding of βmut to SEC1, SEC2, SEC3, and SPEA were 19.8, 7.9, 9.2, and 6.2 μM, respectively. For the binding of βCHO to SEC1, SEC2, and SEC3, the K_Ds were 18.2, 5.4, and 8.5 μM. These results demonstrate that (*a*) the affinity of recombinant Vβ8.2Jβ2.1Cβ1 chain for SEC or SPEA is similar to those of some other T cell surface glycoproteins for their ligands, such as the adhesion molecule CD2 for CD58 and CD48 (25, 26), or of TCRs for peptide/MHC (12, 17, 37, 38) and (*b*) glycosylation does not significantly contribute to the SAG-binding activity of at least this particular β chain.

14.3.d β Chain Binds SEB with Much Lower Affinity than SEC and SPEA. The markedly weaker binding of βmut to SEB than to SEC1 suggested in Fig. 1, *C* and *F* was confirmed by equilibrium binding experiments (Fig. 4). BIAcore measurements were carried out as described above for SEC and SPEA, except that much higher concentrations of β chain (up to 256 μM) were required to approach saturation. The Scatchard plot was linear (r = 0.97) and gave a K_D of 144 μM with predicted maximum binding of 2460 RU (Fig. 4 *D*). Given that about 2700 RU of SEB were immobilized, and that SEB and βmut have similar molecular masses (28.5 and 26.4 kD, respectively), this indicates that >90% of the coupled SAG retained binding activity.

The weak binding of SEB to the 14.3.d β chain was unexpected, particularly in view of the finding that, on a molar basis, this toxin was actually 3- to 10-fold more effective than SEC or SPEA in stimulating the parental 14.3.d T cell hybridoma (Fig. 5). We therefore decided to check our results by an independent technique, sedimentation equilibrium. A major advantage of this method is that both interacting species are in solution, thereby avoiding any possible artefacts arising from ligand immobilization.

The Much Weaker Binding of β chain to SEB than to SEC or SPEA Is Confirmed by Sedimentation Equilibrium. Before analysis of the equilibrium constants for the βmut chain with the various bacterial SAGs, the behavior of the individual receptor fragment and toxins was evaluated in separate sedimentation experiments. All of the species under consideration were well behaved, showing virtually no tendency to aggregate at concentrations up to ~25 μM. An estimate for the molecular weight of the β chain was 28,800, in good agreement with that expected from its amino acid composition (26,400). The molecular weight of SEC3 was determined to be 28,300, compared with an expected value of 28,900. Similar agreement was obtained for SEC1, SEC2 and SEB. However, the molecular weight of SPEA was estimated at only 22,500, somewhat lower than the expected value of 25,800.

The equilibrium dissociation constants determined by sedimentation equilibrium for βmut with various SAGs are presented in Table 1; a representative sedimentation profile is shown in Fig. 6. As can be seen in Table 1, the interaction of the β chain with virtually all the toxins occurs with K_Ds in the low micromolar range (0.9–2.5 μM). An exception is SEB, for which an estimate for the K_D of only 70 μM could be made. However, this estimate should be considered only a lower limit for the actual K_D since, under the feasible conditions for this measurement in the ultracentri-

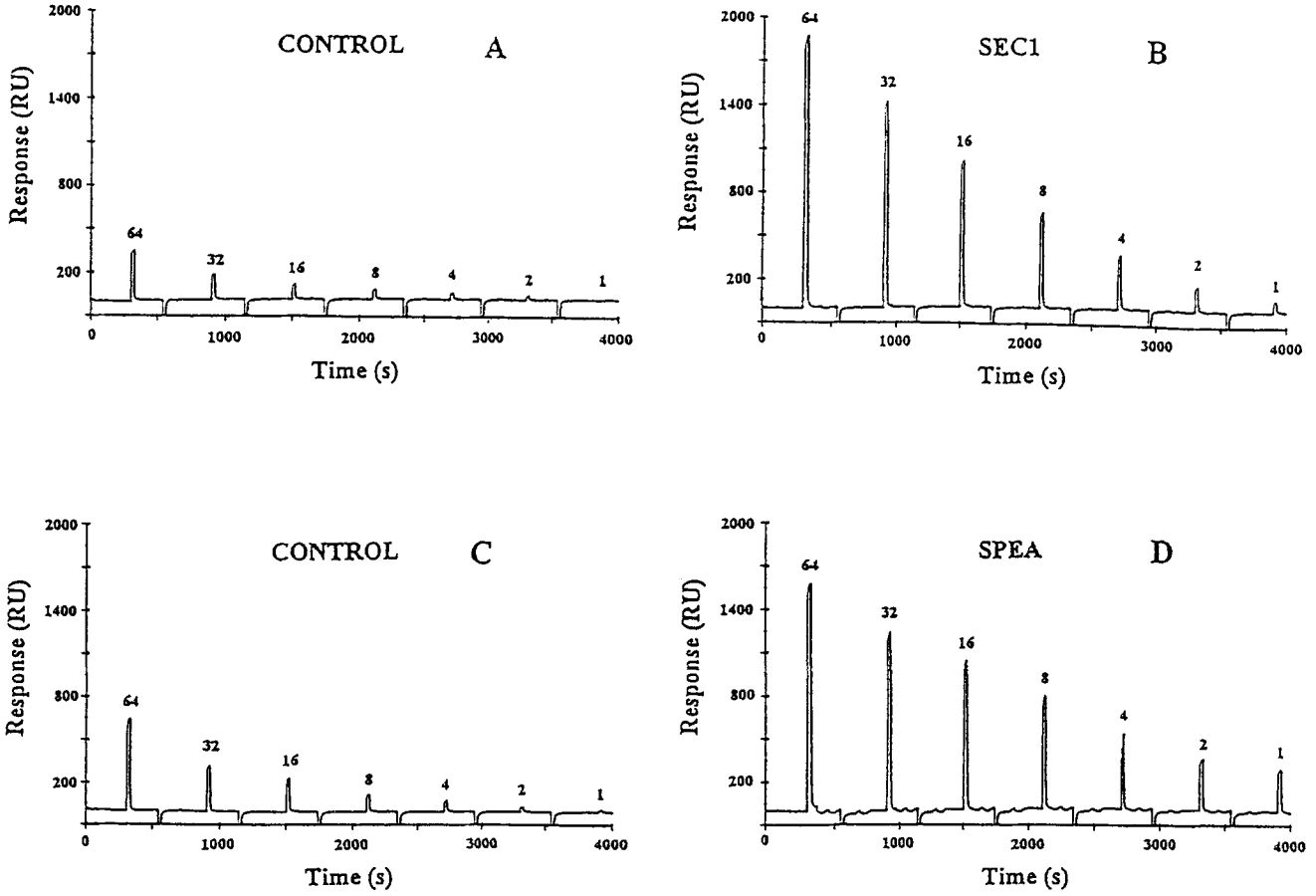

Figure 2. Binding of 14.3.d β chain to immobilized SEC1 and SPEA. βmut was injected at the indicated concentrations (μM) over a control surface with no protein immobilized (*A*), or over ones to which SEC1 (2,050 RU) (*B*) or SPEA (1,350 RU) (*D*) had been coupled. The same concentrations of BSA were also injected over a control surface (*C*). Buffer flow rates were 5 μl/min. Equilibrium binding levels were reached within 4 s. After dissociation with HBS, residual bound protein was eluted using 10-s pulses of 10 mM HCl. Similar profiles were obtained for SEC2 and SEC3.

fuge, weaker binding would not have been detected. Attempts to better define the K_D using 5- and 10-fold higher protein concentrations (up to 0.1 mM) to favor complex formation in this weakly interacting system were unsuccessful due to problems of nonspecific aggregation at these concentrations. It is nevertheless apparent that the SEB binds the 14.3.d β chain with much lower affinity than SEC or SPEA, in agreement with the results from BIAcore.

A comparison of apparent K_D values obtained by sedimentation equilibrium with those from BIAcore reveals that the latter are consistently higher, by up to a factor of 11 in the case of SPEA (Table 1). We believe that the sedimentation equilibrium values more accurately reflect the true binding constants because this method does not involve chemical coupling of ligands to a solid support. In extreme cases (e.g., 26), immobilization can result in complete loss of binding activity, as we observed for β chain coupled to the dextran matrix (see above). Such experiences strongly suggest that intermediate effects on ligand activity are also possible. Indeed, we attribute the generally weaker binding of β chain to SAGs measured by BIAcore than by sedimentation equilibrium to subtle effects on SAG conformation/accessibility arising from the immobilization procedure. These results illustrate the importance of determining binding constants by at least two independent techniques.

Discussion

Our results demonstrate that unglycosylated 14.3.d β chain, whose three-dimensional structure has been determined to high resolution (15), retains the SAG-binding activities of the assembled, glycosylated αβ heterodimer. The ability of the recombinant β chain to specifically bind SEB, SEC1, SEC2, SEC3, and SPEA is consistent with the known proliferative effects of these toxins on Vβ8.2-bearing T cells (2, 36); in contrast, SEA, which does not stimulate cells expressing Vβ8.2 (2), does not bind the 14.3.d β chain with measurable affinity. We therefore conclude that the structure of the β chain, as determined by x-ray crystallography, represents a biologically active conformation of this molecule, at least with respect to those regions responsible for SAG recognition. However, we cannot formally exclude the possibility that other regions of the β chain monomer might have a different conformation when associated with α chain in the αβ heterodimer.

Binding of the 14.3.d β chain to all five SAGs tested is

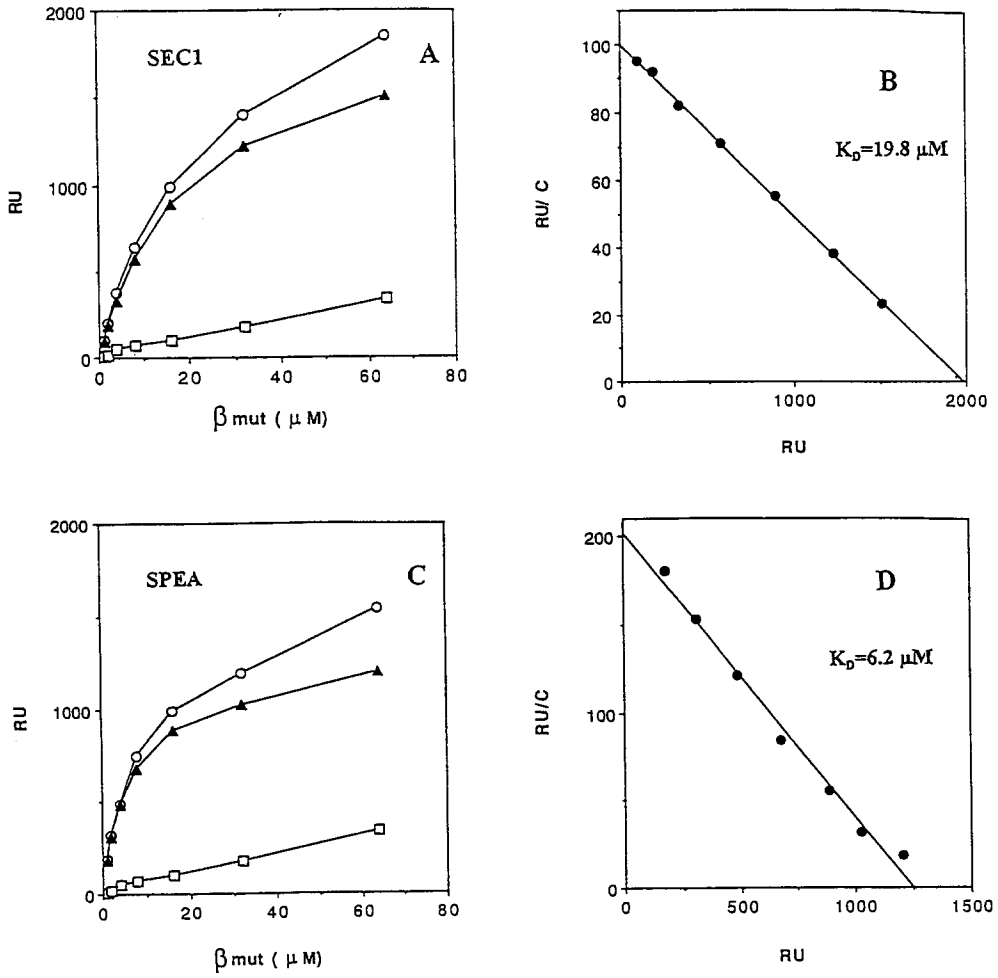

Figure 3. Affinity of 14.3.d β chain for SEC1 and SPEA. Plots are from data in Fig. 2. Responses resulting from injection of the indicated concentrations of βmut over control surface (□, *A*, *C*), SEC1 (○, *A*) and SPEA (○, *C*) are shown. Specific binding (▲, *A*, *C*) was calculated as the difference between the responses for SEC1 and SPEA and the control surface. Scatchard analysis of the specific binding of βmut to SEC1 (*B*) and SPEA (*D*) gave linear plots with correlation coefficients of 0.99 and 0.98, respectively. The apparent K_Ds for the βmut-SEC1 and βmut-SPEA reactions were 19.8 and 6.2 μM, respectively.

characterized by very fast association rates (>1 × 10^5 $M^{-1}s^{-1}$) and extremely fast dissociation rates (>0.1 s^{-1}; Fig. 1); the latter account for the relatively weak affinities observed (i.e., 0.9 μM, at best, in the case of SEC3). Rapid dissociation kinetics have also been reported for the interaction of the rat cell adhesion molecules CD2 and CD48 (25), and for the binding of TCRs to peptide/MHC complexes (37, 38). For adhesion molecules, fast dissociation rates may provide a mechanism to facilitate deadhesion, a requirement for cell motility (26). For TCRs, on the other hand, rapid dissociation rates would not appear to be compatible with the relatively stable interaction with ligand believed to be a prerequisite for signal transduction through the TCR/CD3 complex (38, 39). This suggests that T cell activation by SAGs requires the participation of additional surface molecules to stabilize the transient SAG-TCR interaction, in agreement with other studies (4–8). While class II MHC products have been clearly implicated in this role (1–3, 13), recent evidence (14) indicates that other, yet unidentified, molecules may substitute for MHC in presenting SAGs to T cells (see below). Multivalent binding arising from receptor cross-linking would also effectively decrease the off-rate (and increase the half-time) of the TCR-SAG interaction. Alternatively, rapid dissociation rates may actually be critical for T cell triggering by SAGs, as suggested by a recent study in which a single peptide/MHC complex was found to be able to sequentially bind and trigger nearly 200 TCRs (40).

The complexity of TCR-SAG interactions is further illustrated by the finding that a soluble human TCR expressing the Vβ3.1 gene segment binds SAGs with quite different kinetics than the mouse Vβ8.2 TCR described here (12). Binding of the human Vβ3.1 TCR to SEB is characterized by association and dissociation rates which are only moderately fast: 1.3 × 10^4 $M^{-1}s^{-1}$ and 1.1 × 10^{-2} s^{-1}, respectively. The affinity of this TCR for SEB, however, is comparable to that of the 14.3.d β chain for SEC3: 0.8 μM versus 0.9 μM, respectively. On the other hand, SEB was shown to bind HLA-DR1 with kinetics very similar to those we observe for the Vβ8.2-SAG interaction (12); in both cases, the association and dissociation rates were too rapid to be accurately measured. This implies that binding of human Vβ3.1 to SEB helps stabilize the transient SEB-DR1 interaction and, consequently, the TCR-SEB-DR1 complex (12). We might therefore expect the binding of murine Vβ8.2 to SEB to be stabilized by a more kinetically favorable interaction of SEB with class II molecules (i.e., one with a slower dissociation rate).

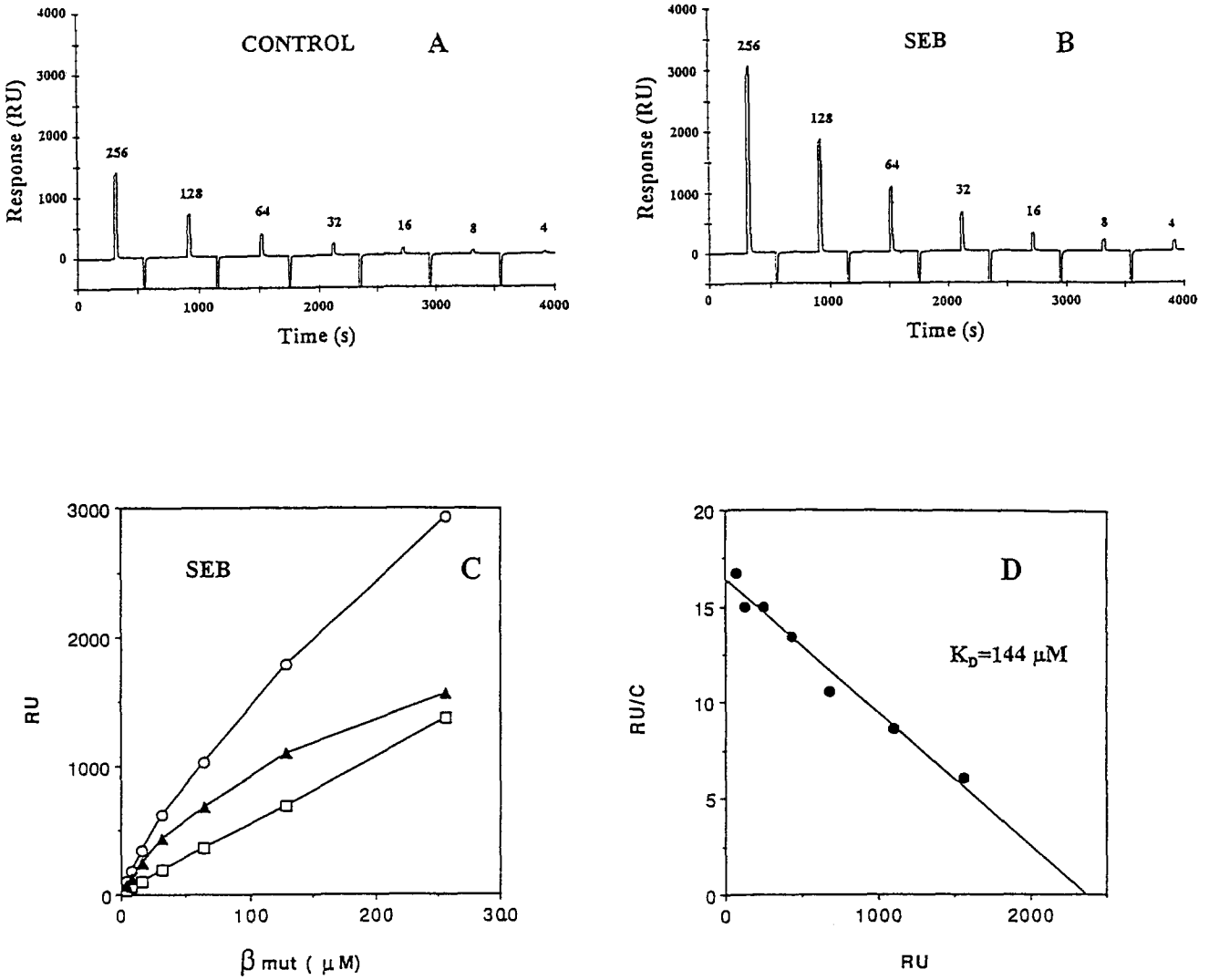

Figure 4. Binding of 14.3.d β chain to immobilized SEB. βmut was injected at the indicated concentrations (μM) over a control surface with no protein immobilized (*A*) or one with 2,700 RU SEB (*B*). Buffer flow rates were 5 μl/min; equilibrium binding levels were reached within 4 s. After dissociation, residual protein was eluted using 10-s pulses of 10 mM HCl. Specific binding (▲, *C*) was calculated as the difference between the total response (○) and the non-specific response (□). The Scatchard plot was linear (r = 0.97) and gave a K_D of 144 μM.

The much weaker binding of the 14.3.d β chain, or of αβ heterodimer, to SEB than to SEC1, SEC2, SEC3 or SPEA was surprising, since all five toxins are known to stimulate Vβ8.2-bearing T cells (2, 36). Furthermore, SEB was considerably more potent than the other toxins in stimulation assays using the 14.3.d hybridoma (Fig. 5). These results may be interpreted in terms of a recent study describing functional differences between SEB and SEC in MHC class II knockout mice (14). Incubation of lymph node cells from class II-deficient mice with SEC, but not SEB, resulted in the clonal expansion of Vβ8-positive T cells and the generation of CTL. Similar results were obtained with SEE, except that Vβ11-positive cells were selectively expanded. The responses to SEC and SEA resembled conventional MHC-associated responses in that T cell bearing the same Vβ elements were specifically affected. Our data provide a straightforward explanation for the finding that activation of Vβ8-positive T cells by SEC can occur in the absence of MHC, in contrast to activation by SEB: whereas SEC1, 2, and 3 bind the 14.3.d β chain with K_Ds of 0.9–2.5 μM, the corresponding value for SEB is between 70 and 140 μM (Table 1). Thus, SEs able to bind TCRs with micromolar affinities may not absolutely require the participation of MHC class II molecules to stabilize their interaction with the β chain. Even in the case of MHC-independent activation, however, APC from MHC class II-deficient mice (or from mice lacking both class I and class II) were required for stimulation (14). This suggests that other surface molecules may substitute for MHC in binding certain SEs, and perhaps also the TCR, thereby helping to stabilize TCR-SE interactions.

A further distinction between SEB and SEC may lie in

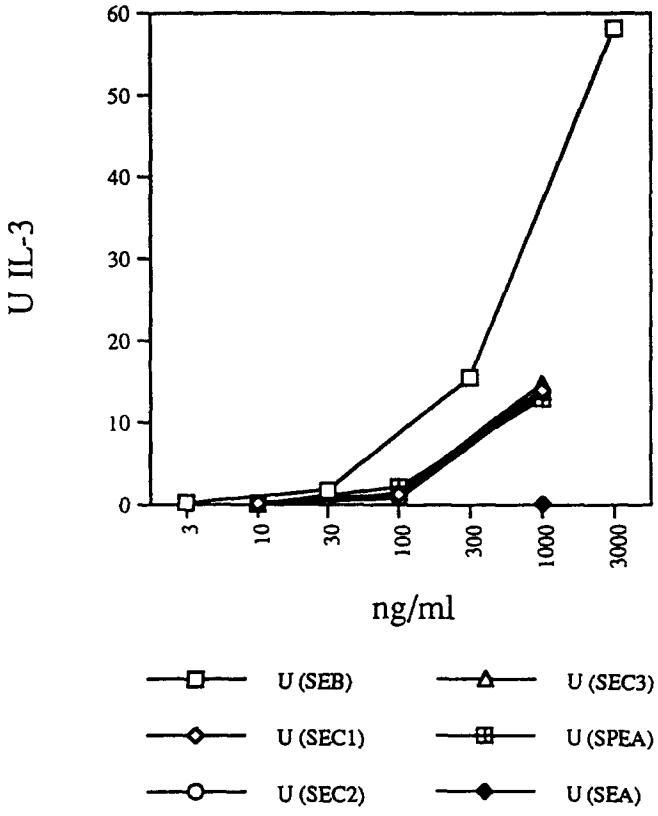

Figure 5. IL-3 production by the parental 14.3.d hybridoma after stimulation with different SAGs in the presence of A20 APC. The SAG concentrations used are as indicated with the different symbols.

their relative affinities for MHC class II. While SEB has been shown to bind HLA-DR1 and -DQ with a K_Ds in the micromolar range (9–11), the data on SEC is less clear. In one study, SEC2 was found able to compete with SEB for

Table 1. *Dissociation Constants for the Binding of Bacterial Toxins to Glycosylated and Unglycosylated 14.3.d β Chain*

SAG	α BIAcore	βCHO BIAcore ($\times 10^{-6}$ M)	βmut BIAcore ($\times 10^{-6}$ M)	βmut Centrifuge ($\times 10^{-6}$ M)
SEC1	NB	18.2	19.8	2.51
SEC2	NB	5.4	7.9	2.32
SEC3	NB	8.5	9.2	0.86
SPEA	NB	ND	6.2	2.11
SEB	NB	ND	144	>70
SEA	NB	NB	NB	ND

Affinity measurements by BIAcore and sedimentation equilibrium were carried out as described in Materials and Methods. All experiments were performed at 25°C using the molecular weight values presented in the text and the specific extinction coefficients provided by Toxin Technology, Inc. The value for the association of SEB with βmut obtained from sedimentation equilibrium is a lower limit for the dissociation constant. *NB*, no detectable binding; *ND*, not done.

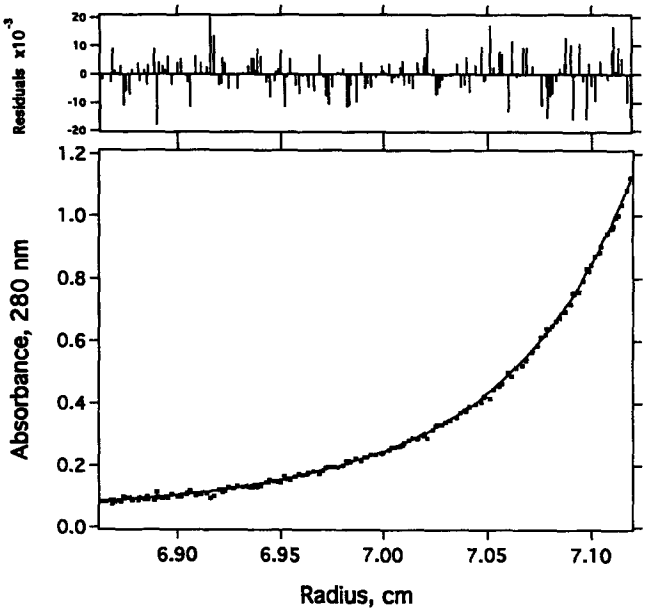

Figure 6. Sedimentation equilibrium of an equimolar mixture of the 14.3.d β chain with SEC1. Sedimentation was performed at 22,000 rpm in 50 mM Tris-HCl, pH 8.0, at 25°C. Starting concentrations of β chain and SEC1 were 7.5 μM. (*Bottom*) Absorbance at 280 nm versus distance from the center of rotation in centimeters. (*Top*) The residuals ($A_{280\ nm}$, theoretical − $A_{280\ nm}$, observed) for the equilibrium between the two components, yielding a K_D of 2.51 μM, are small and random. Similar results were obtained for SEC2, SEC3, and SPEA.

binding to DR1-positive B cells (41), whereas in another study no binding of SEC1 to cells expressing DR3,5 could be demonstrated (42). Indeed, the differential association of certain SAGs with different class II molecules has been put forward as a possible explanation for the lack of an absolute correlation between Vβ expression and SAG reactivity (13).

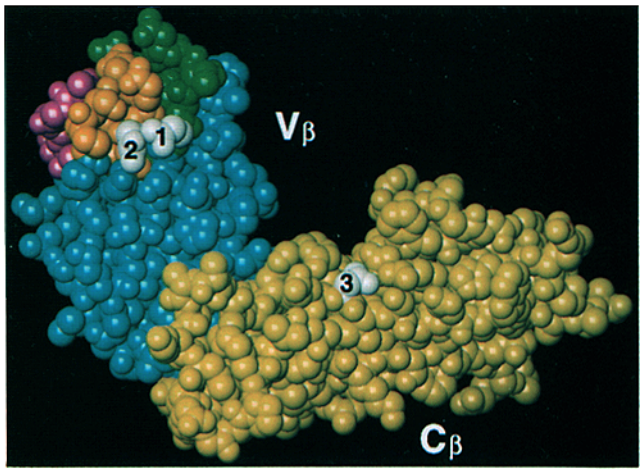

Figure 7. Space-filling model of the 14.3.d β chain showing the location of potential N-linked glycosylation sites. The Vβ and Cβ domains are labeled; CDR1 (residues 25–33) is shown in green, CDR2 (residues 48–56) in purple, and HV4 (residues 69–75) in light brown. The N-linked glycosylation sites at Vβ positions 24 and 74 and at Cβ position 236 are labeled 1, 2, and 3, respectively. Those at Cβ positions 121 and 186 are not visible in this orientation.

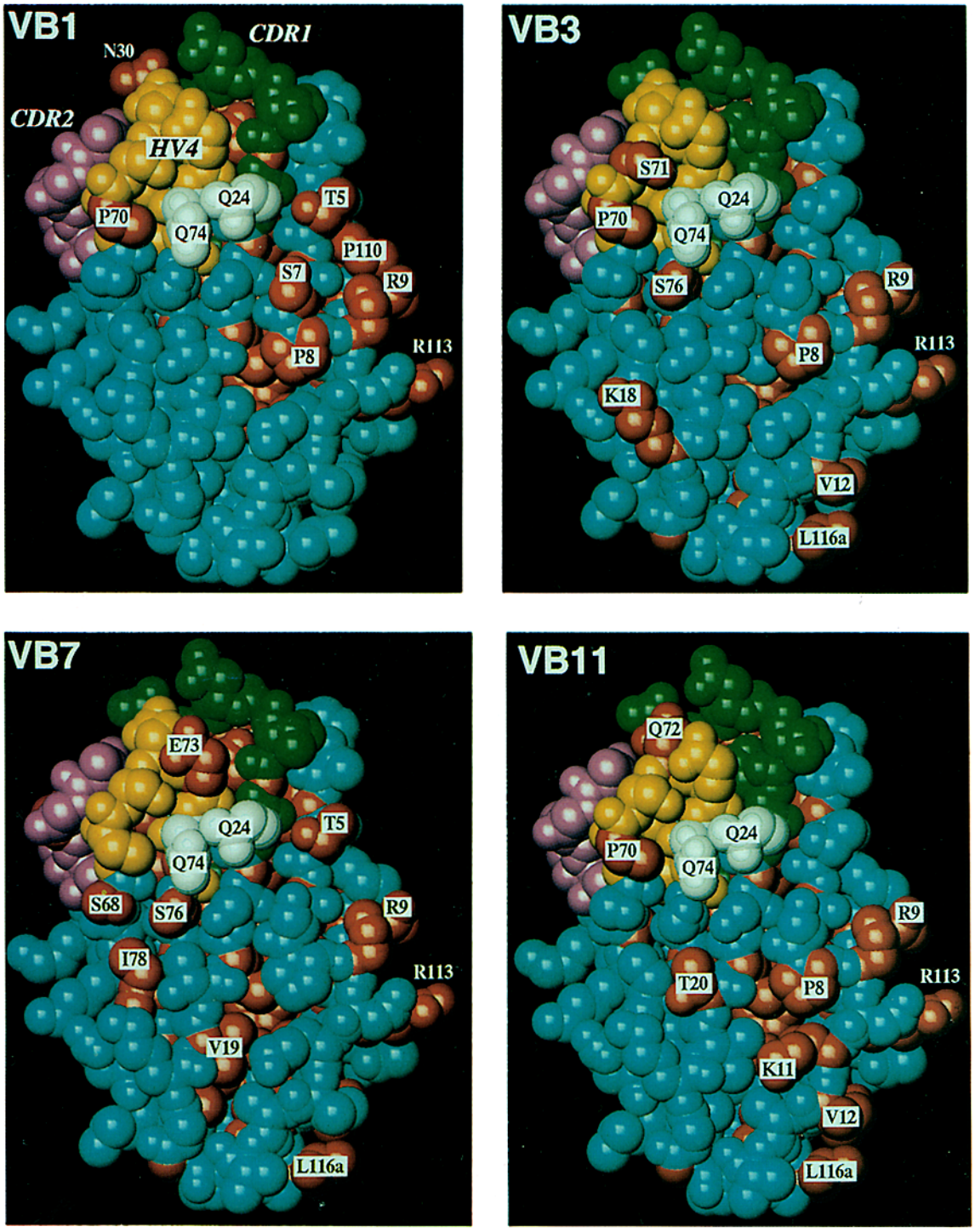

Figure 8. Space-filling model of the putative SAG-binding face of the Vβ8.2 domain showing the location of conserved residues relative to Vβ1, Vβ3, Vβ7, and Vβ11. The amino acid sequences of Vβ segments 1, 3, 7, and 11 were aligned with that of Vβ8.2 according to reference 21; no insertions or deletions with respect to Vβ8.2 were present. Vβ8.2 residues which are conserved relative to each of the other Vβ segments are shown in red in the panels marked Vβ1, Vβ3, Vβ7, and Vβ11. CDR1 is in green, CDR2 in purple, and HV4 in light brown. The potential N-linked glycosylation sites at Vβ8.2 positions 24 and 74 are in gray; neither site is conserved in any of the other Vβ segments. Single-letter abbreviations for amino acid residues are: *E*, Glu; *I*, Ile; *K*, Lys; *L*, Leu; *N*, Asn; *P*, Pro; *Q*, Gln; *R*, Arg; *S*, Ser; *T*, Thr; and *V*, Val.

While no affinities have been reported for the interaction of SAGs with mouse class II proteins, it tempting to speculate that the very weak binding of SEB to Vβ8.2 we observe is compensated by a fairly strong association between SEB and mouse class II, hence accounting for the fact that T cell activation by SEB requires MHC (6). Conversely, SEC, even though it may lack appreciable affinity for mouse class II, binds Vβ8.2 sufficiently tightly to enable it to stim-

ulate T cells independently of MHC. Yet a third scenario is suggested by SEB, which binds both human Vβ3.1 and DR with micromolar affinities (12). Thus, the same enterotoxin may activate different T cells by different mechanisms, depending on the particular Vβ element they express and on the specific MHC background of the host.

As shown in Table 1, glycosylated 14.3.d β chain binds SEC1, 2, and 3 with essentially the same affinity as unglycosylated β chain. This indicates that carbohydrate does not contribute to SAG binding, at least in this particular case. This result is somewhat surprising since the potential N-linked glycosylation sites at Vβ residues Asn24 and Asn74, which were mutated to glutamine (15), are at or near the putative SAG binding site in the three-dimensional structure of the β chain (Fig. 7). In particular, Asn74 is part of the so called fourth hypervariable region (HV4), which has been directly implicated in SAG recognition (3), while Asn24 would be expected to lie adjacent to Asn74 in the unmutated structure. One explanation for the lack of effect of mutations at these positions is that neither Asn24 nor Asn74 is actually glycosylated. We consider this unlikely, as both residues are located on the surface of the protein. Alternatively, these residues may in fact lie at the periphery of the combining site for bacterial SAGs. It is worth noting in this respect that mutation of Asn24 to glutamate has been shown to confer reactivity to Mls-1 (43). This suggests that viral and bacterial SAGs bind somewhat different regions of the Vβ domain.

To investigate the structural basis for the SAG-binding specificity of different β chains, pairwise comparisons were carried out between mouse Vβ8.2 and Vβ1, Vβ3, Vβ7, and Vβ11 based on the crystal structure of the Vβ8.2 domain (Fig. 8). While Vβ3, Vβ7, Vβ8.2, and Vβ11 all react with SEC (and Vβ3, Vβ7, and Vβ8.2 react with SEB as well), Vβ1 does not react with either SEB or SEC, but only with SEA, which does not bind Vβ8.2 (2). As might be expected, a comparison of conserved residues on the putative SAG-binding face of the Vβ8.2 domain reveals that Vβ1 indeed has fewer residues in common with Vβ8.2 than do Vβ3, Vβ7, or Vβ11. Excluding residues unlikely to be involved in direct contacts with bacterial SAGs because they lie at the periphery of this surface (Thr5, Arg9, Val12, Asn30, Pro110, Arg113, and Leu116a), Vβ8.2 shares five residues with Vβ3 (Pro8, Lys18, Pro70, Ser71, and Ser76), five residues with Vβ7 (Val19, Ser68, Glu73, Ser76, and Ileu78), five residues with Vβ11 (Pro8, Lys11, Thr20, Pro70, and Gln72), but only three residues with Vβ1 (Ser7, Pro8, and Pro70). What is remarkable, however, is that even between Vβ8.2 and Vβ3, Vβ7, or Vβ11, all of which react with a similar spectrum of SAGs, the number of common residues is relatively small; furthermore, these residues are not particularly concentrated in HV4. This indicates that certain SAGs (SEC3, for example, which reacts with Vβ3, Vβ7, and Vβ8.2) are able to recognize very different molecular surfaces present on different Vβ domains. One way this could occur is if a single SAG possessed several distinct Vβ-binding sites. However, a recent x-ray crystallographic study of an idiotope–anti-idiotope complex (44) suggests that it is not necessary to postulate multiple binding sites to explain the recognition of topographically different surfaces by a single molecular species. In this study, the contacts made between an anti-lysozyme antibody (D1.3) and an anti-idiotopic antibody (E5.2) raised against it were compared with the contacts made between D1.3 and lysozyme in the original antigen–antibody complex (45). Surprisingly, it was found that D1.3 employed essentially the same set of combining site residues (and most of the same atoms) in binding lysozyme as in binding E5.2, despite the fact that the sites on lysozyme and E5.2 recognized by D1.3 were structurally unrelated. Whether similar mechanisms operate to permit individual SAGs to interact with a number of different Vβ families must await direct structural studies of β chain-SAG complexes.

We are grateful to Michael Robinson (Pharmacia Biosensor) for invaluable advice and discussions throughout the course of this work.

This research was supported by National Institutes of Health (NIH) grant AI36900 and a grant from the Richard Lounsbery Foundation (R. A. Mariuzza), NIH grant RR08937 (E. Eisenstein), NIH grant HL36611 (P. M. Schlievert), and grants from the Kimberly-Clark Corporation, (Neenah, WI), the Personal Products Co. (New Brunswick, NJ), and Tambrands (Palmer, MA) (P.M. Schlievert and D.H. Ohlendorf). Support from the Lucille P. Markey Charitable Trust is also gratefully acknowledged. The Basel Institute for Immunology was founded and is supported by F. Hoffmann-LaRoche Ltd., Basel, Switzerland.

E. L. Malchiodi is a Fellow of CONICET, Argentina.

Address correspondence to Dr. Roy A. Mariuzza, Center for Advanced Research in Biotechnology, 9600 Gudelsky Drive, Rockville, MD 20850.

Received for publication 11 May 1995 and in revised form 10 July 1995.

Note added in proof: Since this manuscript was submitted, we have determined the crystal structure of a complex between the 14.3.d β chain and SEC3. Superantigen contacts are mainly with CDR1, CDR2, and HV4, rather than with framework residues. The glycosylation sites at Vβ positions 24 and 74 are not directly implicated in the β chain-SEC3 interface.

References

1. Janeway, C.A., Jr., J. Yagi, P.J. Conrad, M.E. Katz, B. Jones, S. Vroegop, and S. Buxser. 1989. T cell responses to Mls and to bacterial proteins that mimic its behavior. *Immunol. Rev.* 107:61–88.
2. Marrack, P., and J. Kappler. 1990. The staphylococcal enterotoxins and their relatives. *Science (Wash. DC).* 248:705–711.
3. Klotzin, B.L., D.Y.M. Leung, J. Kappler, and P. Marrack. 1993. Superantigens and their potential role in human disease. *Adv. Immunol.* 54:99–166.
4. Carlsson, R., H. Fischer, and H.O. Sjogren. 1988. Binding of staphylococcal enterotoxin A to accessory cells is a requirement for its ability to activate human T cells. *J. Immunol.* 120: 92–101.
5. Fleischer, B., H. Schrezenmeier, and H. Conradt. 1989. T lymphocyte activation by staphylococcal enterotoxins: role of class II molecules and cell surface structures. *Cell. Immunol.* 144:892–901.
6. White, J., A. Herman, A.M. Pullen, R. Kubo, J.W. Kappler, and P. Marrack. 1989. The Vβ-specific staphylococcal enterotoxin B: stimulation of mature T cells and clonal deletion in neonatal mice. *Cell.* 56:27–35.
7. Yagi, J., J. Baron, S. Buxser, and C.A. Janeway, Jr. 1990. Bacterial proteins that mediate the association of a defined subset of T cell receptor: CD4 complexes with class II MHC. *J. Immunol.* 144:892–901.
8. Gascoigne, N.R.J., and K.T. Ames. 1991. Direct binding of secreted T-cell receptor β chain to superantigen associated with class II major histocompatibility complex protein. *Proc. Natl. Acad. Sci. USA.* 88:613–616.
9. Fraser, J.D. 1989. High-affinity binding of staphylococcal enterotoxins A and B to HLA-DR. *Nature (Lond.).* 339:221–223.
10. Scholl, P.R., A. Diez, and R.S. Geha. 1989. Staphylococcal enterotoxin B and toxic shock syndrome toxin-1 bind to distinct sites on HLA-DR and HLA-DQ molecules. *J. Immunol.* 143:2583–2588.
11. Fischer, H., M. Dohlsten, M. Lindvall, H.O. Sjogren, and R. Carlsson. 1989. Binding of staphylococcal enterotoxin A to HLA-DR on B cell lines. *J. Immunol.* 142:3153–3157.
12. Seth, A., L.J. Stern, T.H.M. Ottenhoff, I. Engel, M.J. Owen, J.R. Lamb, R.J. Klausner, and D.C. Wiley. 1994. Binary and ternary complexes between T-cell receptor, class II MHC and superantigen *in vitro*. *Nature (Lond.).* 369:324–327.
13. Woodland, D.L., and M.A. Blackman. 1993. How do T-cell receptors, MHC molecules and superantigens get together? *Immunol. Today* 14:208–212.
14. Avery, A.C., J.S., Markowitz, M.J. Grusby, L.H. Glimcher, and H. Cantor. 1994. Activation of T cells by superantigen in class II-negative mice. *J. Immunol.* 153:4853–4861.
15. Bentley, G.A., G. Boulot, K. Karjalainen, and R.A. Mariuzza. 1995. Crystal structure of the β chain of a T cell antigen receptor. *Science (Wash. DC).* 267:1984–1987.
16. Bohach, G.A., D.J. Fast, R.D. Nelson, and P.M. Schlievert. 1990. Staphylococcal and streptococcal pyrogenic toxins involved in toxic shock syndrome and related illnesses. *Crit. Rev. Microbiol.* 17:251–272.
17. Weber, S., A. Traunecker, F. Oliveri, W. Gerhard, and K. Karjalainen. 1992. Specific low-affinity recognition of major histocompatibility complex plus peptide by soluble T-cell receptor. *Nature (Lond.).* 356:793–796.
18. Taylor, A.H., A.M. Haberman, W. Gerhard, and A.J. Caton. 1990. Structure-function relationships among highly diverse T cells that recognize a determinant from influenza virus hemagglutinin. *J. Exp. Med.* 172:1643–1651.
19. Traunecker, A., B. Dolder, and K. Karjalainen. 1991. Myeloma based expression system for production of large mammalian proteins. *Trends Biotech.* 9:109–113.
20. Boulot, G., G.A. Bentley, K. Karjalainen, and R.A. Mariuzza. 1994. Crystallization and preliminary X-ray diffraction analysis of the β chain of a T-cell antigen receptor. *J. Mol. Biol.* 235:795–797.
21. Kabat, E.A., T.T. Wu, H.M. Perry, K.S. Gottesman, and C. Foeller. 1991. Sequences of Proteins of Immunological Interest. 5th ed. (Public Health Services, National Institutes of Health, Washington, DC).
22. Kubo, R.T., W. Born, J.W. Kappler, P. Marrack, and M. Pigeon. 1989. Characterization of a monoclonal antibody which detects all murine αβ T cell receptors. *J. Immunol.* 142:2736–2742.
23. Ward, E.S. 1992. Secretion of T cell receptor fragments from recombinant *Escherichia coli* cells. *J. Mol. Biol.* 224:885–888.
24. Fields, B.A., X. Ysern, R.J. Poljak, X. Shao, E.S. Ward, and R.A. Mariuzza. 1994. Crystallization and preliminary X-ray diffraction study of a bacterially produced T-cell antigen receptor Vα domain. *J. Mol. Biol.* 239:339–341.
25. van der Merwe, P.A., M.H. Brown, S.J. Davis, and A.N. Barclay. 1993. Affinity and kinetic analysis of the interaction of the cell adhesion molecules rat CD2 and CD48. *EMBO (Eur. Mol. Biol. Organ.) J.* 12:4945–4954.
26. van der Merwe, P.A., A.N. Barclay, D.W. Mason, E.A. Davies, B.P. Morgan, M. Tone, A.K.C. Krishnam, C. Ianelli, and S.J. Davis. 1994. Human cell-adhesion molecule CD2 binds CD58 (LFA-3) with a very low affinity and an extremely fast dissociation rate but does not bind CD48 or CD59. *Biochemistry.* 33:10149–10160.
27. Johnsson, B., S. Lofas, and G. Lindquist. 1991. Immobilization of proteins to a carboxymethyldextran modified gold surface for biospecific interaction analysis in surface plasmon resonance. *Anal. Biochem.* 198:268–277.
28. Karlsson, R., A. Michaelsson, and L. Mattson. 1991. Kinetic analysis of monoclonal antigen-antibody interactions with a new biosensor based analytical system. *J. Immunol. Methods.* 145:229–240.
29. Johnson, M.L., J.J. Correia, D.A. Yphantis, and H.R. Halvorson. 1981. Analysis of data from the analytical ultracentrifuge by nonlinear least-squares techniques. *Biophys. J.* 36: 575–588.
30. Brooks, I.S., K.K. Soneson, and P. Hensley. 1993. Development of a MAC based data analysis package for equilibrium sedimentation data from the analytical ultracentrifuge. *Biophys. J.* 64:A244.
31. Brooks, I., R. Wetzel, W. Chan, G. Lee, D.G. Watts, K.K. Soneson, and P. Hensley. 1994. Association of REI immunoglobulin light chain V_L domains: the functional linearity of parameters in equilibrium analytical ultracentrifugation models for self-associating systems. *In* Modern Analytical Ultracentrifugation. Acquisition and Interpretation of Data for Biological and Synthetic Polymer Systems. T.M. Schuster and T.M. Laue, editors. Birkhauser, Boston. 15–36.
32. Roark, D.E. 1976. Sedimentation equilibrium techniques: multiple speed analysis and an overspeed procedure. *Biophys. Chem.* 5:185–196.
33. Johnson, M.L., and S.G. Fraser. 1985. Nonlinear least-squares

analysis. *Methods Enzymol.* 117:301–342.
34. Brocker, T., A. Peter, A. Traunecker, and K. Karjalainen. 1993. New simplified molecular design for functional T cell receptor. *Eur. J. Immunol.* 23:1435–1439.
35. Granzow, R., and R. Reed. 1992. *Biotechnology.* 10:390–393.
36. Imanishi, K., H. Igarashi, and T. Uchiyama. 1990. Activation of murine T cells by streptococcal pyrogenic exotoxin A. *J. Immunol.* 145:3170–3176.
37. Matsui, K., J.J. Boniface, P. Steffner, P.A. Reay, and M.M. Davis. 1994. Kinetics of T-cell receptor binding to peptide/I-E^k complexes: correlation of the dissociation rate with T-cell responsiveness. *Proc. Natl. Acad. Sci. USA.* 91:12862–12866.
38. Corr, M., A.E. Slanetz, L.F. Boyd, M.T. Jelonek, S. Khilko, B.K. Al-Ramidi, Y.S. Kim, S.E. Maher, A.L.M. Bothwell, and D.H. Margulies. 1994. T cell receptor-MHC class I peptide interactions: affinity, kinetics, and specificity. *Science (Wash. DC).* 265:946–948.
39. Germain, R.N. 1994. MHC-dependent antigen processing and peptide presentation: providing ligands for T lymphocyte activation. *Cell.* 76:287–299.
40. Valitutti, S., S. Muller, M. Cella, E. Padovan, and A. Lanzavecchia. 1995. Triggering of a large number of T cell receptors by a small number of peptide-MHC complexes. *Nature (Lond.).* 375:148–151.
41. Hewitt, C.R.A., J.R. Lamb, J. Hayball, M. Hill, M.J. Owen, and R.E.O. O'Hehir. 1992. Major histocompatibility complex independent clonal T cell anergy by direct interaction of *Staphylococcal aureus* enterotoxin B with the T cell antigen receptor. *J. Exp. Med.* 175:1493–1499.
42. Fraser, J.D., R.G. Urban, J.L. Strominger, and H. Robinson. 1992. Zinc regulates the function of two superantigens. *Proc. Natl. Acad. Sci. USA.* 89:5507–5511.
43. Pullen, A.M., T. Wade, P. Marrack, and J.W. Kappler. 1990. Identification of the region of T cell receptor β chain that interacts with the self-superantigen Mls-1^a. *Cell.* 61:1365–1374.
44. Fields, B.A., F.A. Goldbaum, X. Ysern, R.J. Poljak, and R.A. Mariuzza. 1995. Molecular basis of antigen mimicry by an anti-idiotope. *Nature (Lond.).* 374:739–742.
45. Amit, A.G., R.A. Mariuzza, S.E.V. Phillips, and R.J. Poljak. 1986. The three-dimensional structure of an antigen-antibody complex at 2.8 Å resolution. *Science (Wash. DC).* 233: 747–753.